

Gene Transfer of Brain-derived Neurotrophic Factor (BDNF) Prevents Neurodegeneration Triggered by FXN Deficiency

Yurika Katsu-Jiménez^{1,2}, Frida Loría^{1,2}, Juan Carlos Corona^{1,2,3} and Javier Díaz-Nido^{1,2}

¹Centro de Biología Molecular Severo Ochoa (UAM-CSIC) and Departamento de Biología Molecular, Universidad Autónoma de Madrid (UAM), Madrid, Spain; ²Instituto de Investigaciones Sanitarias Hospital Puerta de Hierro-Majadahonda (IDIPHIM), Madrid, Spain; ³Current address: Hospital Infantil de México "Federico Gómez", México, D.F., México

Friedreich's ataxia is a predominantly neurodegenerative disease caused by recessive mutations that produce a deficiency of frataxin (FXN). Here, we have used a herpesviral amplicon vector carrying a gene encoding for brain-derived neurotrophic factor (BDNF) to drive its overexpression in neuronal cells and test for its effect on FXN-deficient neurons both in culture and in the mouse cerebellum *in vivo*. Gene transfer of BDNF to primary cultures of mouse neurons prevents the apoptosis which is triggered by the knockdown of FXN gene expression. This neuroprotective effect of BDNF is also observed *in vivo* in a viral vector-based knockdown mouse cerebellar model. The injection of a lentiviral vector carrying a minigene encoding for a FXN-specific short hairpin ribonucleic acid (shRNA) into the mouse cerebellar cortex triggers a FXN deficit which is accompanied by significant apoptosis of granule neurons as well as loss of calbindin in Purkinje cells. These pathological changes are accompanied by a loss of motor coordination of mice as assayed by the rota-rod test. Coinjection of a herpesviral vector encoding for BDNF efficiently prevents both the development of cerebellar neuropathology and the ataxic phenotype. These data demonstrate the potential therapeutic usefulness of neurotrophins like BDNF to protect FXN-deficient neurons from degeneration.

Received 11 September 2015; accepted 21 January 2016; advance online publication 15 March 2016. doi:10.1038/mt.2016.32

INTRODUCTION

Friedreich's ataxia (FRDA; [OMIM 229300]) is a predominantly neurodegenerative disease with a very early onset and mainly affects neurons at the dorsal root ganglia, spinal cord, brainstem, and cerebellum.^{1–5} Many patients also develop a hypertrophic cardiomyopathy, skeletal deformities, and diabetes.^{1,2} The disease is caused by mutations in the nuclear FXN gene [MIM 606829], located on chromosome 9q13 which encodes for a protein called frataxin (FXN). The most common mutation is an expansion of a guanine adenine adenine (GAA) triplet located in the first intron of the gene which leads to a decreased FXN mRNA transcription and consequently a reduced amount of the functional protein that

can reach levels below 25–30%.^{6–8} FXN is a predominantly mitochondrial protein with a ubiquitous distribution and is enriched in tissues with a high content of mitochondria, such as the brain, heart, pancreas, skeletal muscle, liver, and brown adipose tissue.⁹ It appears that FXN is involved in the biogenesis and repair of iron-sulfur clusters and therefore performs a key role in the regulation of iron homeostasis and mitochondrial functions.^{10–13}

Different experimental models are being used both to study the physiopathology of FRDA and the development of novel therapeutic approaches. Mouse models and relevant human cells are particularly relevant in this respect. Mouse models include mice with full deletion of the FXN gene and mice with a diminished FXN expression as the consequence of bearing a FXN transgene with a GAA expansion.¹⁴ Human cell models include antisense, ribozyme, small interfering RNA, and short-hairpin RNA-based cell lines as well as FRDA patient-derived cells.¹⁴ Human neural cell models are providing important insights into the molecular mechanisms underlying neurodegeneration in FRDA. Thus, the activation of the intrinsic caspase-3-dependent apoptotic cell death pathway has been observed in human neuron-like cells derived from neuroblastoma cells after FXN gene knockdown, as well as in human neurons derived from FRDA patient-derived induced pluripotent stem cells.^{15,16} Furthermore, cultured mouse neurons exposed to a soluble factor released from FXN-deficient astrocytes also exhibit an increased apoptosis.¹⁷ Thus, the activation of neuronal apoptosis in response to both an intrinsic mitochondrial dysfunction and an altered secretome from FXN-deficient glial cells may contribute to neurodegeneration in FRDA.¹⁷

Accordingly, the use of drugs or genes able to prevent neuronal apoptosis may be a plausible therapeutic approach for FRDA in a similar way to what has been suggested for other neurodegenerative diseases.¹⁸ Some therapeutic approaches for treating FRDA try to raise FXN levels within cells using either drugs capable of reverting FXN gene silencing or gene therapy.¹⁹ Different gene therapy strategies based on the re-introduction of the normal FXN gene, activation of the silenced gene by artificial transcription factors or excision of the expanded GAA repeats are being investigated.^{20–26} Strategies aimed at blocking the activation of apoptosis in FRDA neurons might be complementary to the approaches based on increasing FXN expression. Interestingly, it

Correspondence: Javier Díaz-Nido, Centro de Biología Molecular Severo Ochoa, Universidad Autónoma de Madrid (UAM), C/Nicolás Cabrera 1, 28049 Madrid, Spain. E-mail: javier.diaznido@uam.es

has been suggested that therapies targeting cell death pathways downstream of disease triggers may provide good opportunities to treat neurodegenerative disease.¹⁸ Neurotrophic factors are secreted proteins able to block apoptosis and enhance neuronal function.^{27,28} Because of these properties, neurotrophic factors are being assayed as disease-modifying therapies in experimental models of both neurodegenerative diseases and traumatic injuries of the nervous system.^{28–35} Here, we have used primary neuronal cultures treated with a lentiviral vector encoding for a FXN-specific shRNA and a new mouse model based on the intracerebellar injection of this vector. Our results with these models constitute a proof of principle about the possibility of using neurotrophins like brain-derived neurotrophic factor (BDNF) as a therapeutic option for neurodegeneration in FRDA.

RESULTS

Effect of neurotrophic factors on the apoptotic cell death of cultured neurons after FXN gene knockdown

In order to obtain FXN-deficient neurons, we used primary cultures of neurons from mouse 17-day embryonic cerebral cortices, in which we knocked down FXN gene expression by transduction with a lentiviral vector encoding a short-hairpin RNA sequence against FXN (shRNA-37).¹⁵ We used as a control a lentivector containing a random scrambled shRNA sequence (shRNA-sc).¹⁵ We observed that, 72 hours post-transduction, shRNA-37 induced a decrease of FXN protein levels to 25% of those found in control neurons, as shown in western-blot (Figure 1a,b). In parallel, the viability of cultured neurons decreased with the decrease of FXN protein level (Figure 1c). At 72 hours post transduction the cell viability of FXN-deficient neurons was around 60% of the total cells, while no changes were observed in neurons treated with a scrambled interference sequence (shRNA-sc). Since at 72 hours post transduction FXN protein levels were similar to those found in FRDA patients, we used this time point for the rest of experiments.

In order to characterize the cell death of neurons in response to FXN deficiency, caspase-3 activation, as a marker of apoptosis, was analyzed by western blotting.³⁶ We observed a strong caspase-3 activation that paralleled both the increased cell death and the decrease in FXN levels in shRNA-37-transduced neurons (Figure 1d,e). Furthermore, the cell death was significantly reduced in the presence of the pan-caspase inhibitor Q-VD-OPh (*N*-(2-Quinolyl)-valyl-aspartyl-(2,6-difluorophenoxy)methyl ketone) (Figure 1f). These results indicate that FXN-deficient neurons die through apoptosis, in agreement with previous results obtained with human neurons derived from either neuroblastoma cell or induced pluripotent stem cells.^{15,16}

The apoptotic death of cultured neurons in response to FXN knockdown may be used as an *in vitro* assay to test for the potential of different drugs or genes to prevent neurodegeneration triggered by FXN deficiency. So we have used this *in vitro* assay to test for the effect of the addition of recombinant neurotrophic factors on the survival of FXN-deficient neurons in culture. Primary cultures of mouse neurons were transduced with lentivector shRNA-37, using shRNA-sc as control, in the presence of different recombinant neurotrophic factors (hepatocyte growth

factor, nerve growth factor, neurotrophin-3, neurotrophin-4, and BDNF). We measured cell viability and caspase-3 activation at 72 hours after lentiviral transduction (Figure 2a–c). All neurotrophic factors of the neurotrophin family (nerve growth factor, neurotrophin-3, neurotrophin-4, and BDNF) were able to protect FXN-deficient neurons from apoptosis, BDNF being the most effective. The potency of the different neurotrophins may be correlated with the expression level of their specific tyrosine receptor kinase (Trk). The fact that TrkB is the most abundant in primary cultures of cortical neurons may explain the highest potency of BDNF.

BDNF gene transfer prevents apoptotic cell death of FXN-deficient neurons in culture

The previous results suggest the potential of neurotrophins, particularly BDNF, to enhance the survival of FXN-deficient neurons in culture. However, recombinant neurotrophin proteins have very poor pharmacokinetic properties and are unable to cross the blood–brain barrier which hinders their use *in vivo*. Viral vector-mediated delivery of genes encoding neurotrophic factors has been widely used to increase their levels within the central nervous system (CNS).^{28,33,37} For this reason, we decided to test for the effect of BDNF gene transfer in FXN-deficient neurons in culture.

Cultured cerebral cortex neurons were cotransduced with lentivector shRNA-37, or with shRNA-sc as control, and with herpes simplex virus type 1-derived amplicon vectors (HSV-1) amplicon vectors containing the cDNA of BDNF (HSV-BDNF) or the cDNA of β -galactosidase (HSV-LacZ) as control. BDNF overexpression in FXN-deficient neurons was accompanied by a significant decrease of caspase-3 activation, observed by western blot assay in comparison with FXN-deficient neurons cotransduced with HSV-LacZ (Figure 3a,b). In addition, when BDNF is overexpressed, both the viability and the metabolic activity of FXN-deficient neurons increase significantly up to 100% measured using the calcein/propidium iodide assay to measure cell viability and the MTS reduction assay as an indication of the cell metabolic activity (Figure 3c,d). These data suggest that the treatment with HSV-BDNF was able to prevent cell death induced by the lack of FXN.

To test whether the BDNF neuroprotective effect was mediated by the TrkB receptor, we measured cell viability of FXN-deficient neurons in conditions that interfere with BDNF signaling. Firstly, we cotransduced neurons with the lentivectors and the HSV-1 vectors, in the presence of the TrkB inhibitor K252a (50 μ M).³⁸ We observed that the inhibitor K252a fully reversed the neuroprotective effect of BDNF in FXN-deficient neurons (Figure 4a). As a second approach, BDNF was neutralized with a specific antibody, IgY-BDNF, and in accordance with the previous data we also observed a loss of BDNF protection when compared with the IgY-control condition (Figure 4b). Altogether, these results indicate that BDNF specifically protects FXN-deficient neurons from cell death through activation of TrkB receptors.

In vivo FXN gene knockdown after stereotaxic injection of viral vectors into the cerebellum

In order to obtain an *in vivo* model of FXN knockdown in the cerebellum, we transduced adult mice with the lentivector shRNA-37 (using the lentivector shRNA-sc as control) by stereotaxic

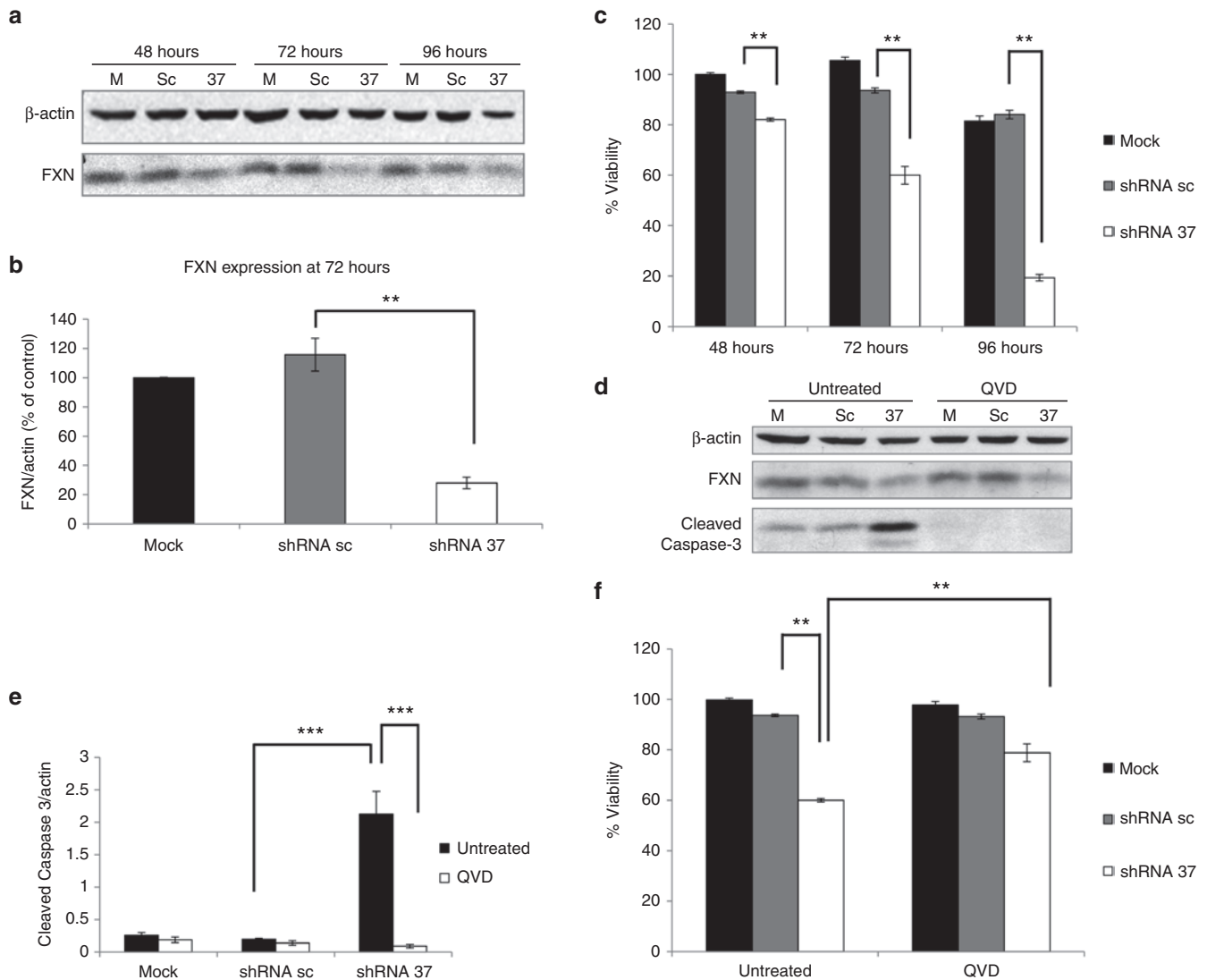


Figure 1 Knockdown of FXN in cultured neurons triggers apoptotic cell death. Primary cortical neurons were transduced with lentivectors encoding for shRNA sequences against human FXN (shRNA-37), or containing a random scrambled shRNA sequence (shRNA-sc), or were left untransduced as an untreated control. **(a)** Representative western-blot analysis of FXN expression at 48, 72, and 96 hours post-transduction in comparison with that found in untransduced cells (mock, m). **(b)** Densitometric analysis of FXN levels in cultured neurons reveals significant differences at 72 hours post-transduction. **(c)** Cell viability of cultured neurons was estimated at 48, 72, and 96 hours post-transduction. **(d)** Western-blot analysis of FXN and cleaved caspase-3 at 72 hours post-transduction in the absence or presence of 50 μ M Q-VD-OPH (*N*-(2-Quinoly)-valyl-aspartyl-(2,6-difluorophenoxy) methyl ketone). **(e)** Quantification of cleaved caspase-3 levels in FXN-deficient neurons shows significant differences at 72 hours post-transduction. **(f)** Cell viability of cultured neurons at 72 hours post-transduction in the absence or presence of 50 μ M Q-VD-OPH (QVD). Significant differences were shown between FXN-deficient neurons with or without QVD. Data represent mean values \pm SEM from three independent experiments, ** $P \leq 0.005$, *** $P \leq 0.0005$.

injection at coordinates AP -6.5 mm; lateral 1 mm; V -2.5 mm (Figure 5a,b).³⁹ A sub-group of mice injected with shRNA-37 was coinjected either with the HSV-BDNF amplicon vector, or with the HSV-LacZ amplicon vector as control. Thus, we obtained four different groups of animals, which will be named for further references as *sham*, *sc*, *37 + HSV-LacZ*, and *37 + HSV-BDNF* (Figure 5c). With this procedure FXN protein levels in the cerebellum of shRNA-37-infected animals decrease to 30% 4 days after the operation, analyzed by western blot assay (Figure 5d,e). We observed a significantly increased expression of BDNF in the *37 + HSV-BDNF* group, measured by enzyme-linked immunosorbent assay (ELISA) assay (Figure 5f).

BDNF prevents apoptotic cell death of FXN-deficient cerebellar neurons *in vivo*

To gain further insight into the viability of BDNF gene transfer as a therapeutic approach for FRDA, we tested for its effect *in vivo*. In this study, we analyzed cerebella of the four experimental groups of animal: *sham*, *sc*, *37 + HSV-LacZ*, and *37 + HSV-BDNF* (Figure 5c). Analyzing several histological sections from the cerebella of the different groups of animals, we were not able to distinguish any notable differences in the cytoarchitecture of the cerebellar cortex. Thus, we decided to test for different apoptotic markers to further investigate FXN-deficient cerebella *in vivo*. We observed in FXN-deficient cerebella a significant increase of

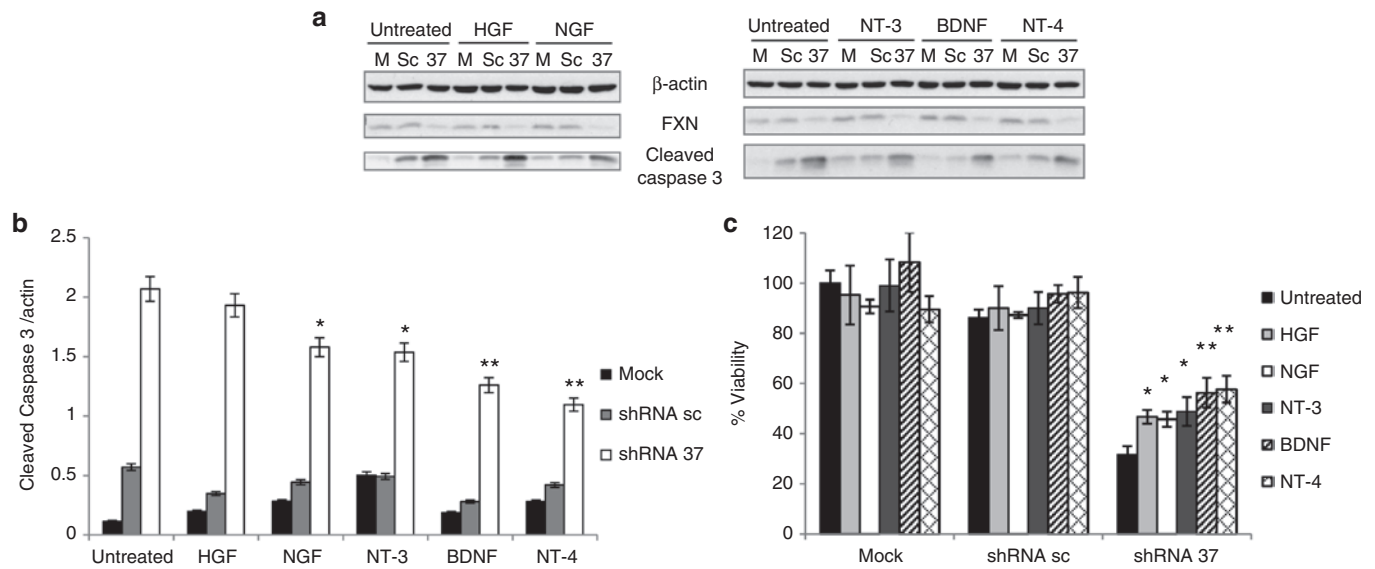


Figure 2 Effects of recombinant human neurotrophic factors in FXN-deficient neurons in culture. Primary cortical neurons were transduced with lentivectors (shRNA-sc or shRNA-37) or were left untransduced as a mock control (m), in the presence of different trophic factors such as hepatocyte growth factor (HGF), neurotrophin-3 (NT-3), neurotrophin-4 (NT-4) and brain-derived neurotrophic factor (BDNF) (100 ng/ml) and nerve growth factor (NGF) (1 μ g/ml). **(a)** Representative western-blot analysis of FXN and cleaved caspase-3 levels at 72 hours upon transduction and treatments. **(b)** Quantification of cleaved caspase-3 levels in FXN-deficient neurons upon transduction reveals a decrease of caspase-3 activation when cells were treated with neurotrophins compared to untreated cells. **(c)** Cell viability of cultured neurons at 72 hours upon transduction shows significant differences between FXN-deficient neurons with neurotrophins compared to untreated cells. Data represent mean values \pm SEM from three independent experiments, * $P \leq 0.05$, ** $P \leq 0.005$.

activated caspase-3 by western blot assay, which was not observed when BDNF was overexpressed (Figure 6b,c). We also examined some protein substrates for caspase-3, including cleaved Poly [ADP-ribose] polymerase 1 (PARP 1).⁴⁰ An increase of cleaved PARP 1 was detected by western blot in FXN-deficient cerebella, and again the overexpression of BDNF significantly protected against PARP 1 cleavage (Figure 6b,d). Furthermore, we found by immunohistochemistry that FXN-deficient cerebellar granule neurons were positive for fractin, which is the N-terminal fragment of actin which results from caspase-3 cleavage. No other cell type showed a positive result for fractin marker in FXN-deficient cerebella. When FXN-deficient neurons were treated with HSV-BDNF, the number of fractin-positive cerebellar granule cells significantly decreased (Figure 6a). This indicates that HSV-BDNF prevents the apoptotic cell death of FXN-deficient cerebellar granule neurons *in vivo*.

BDNF prevents the loss of calbindin in FXN-deficient cerebellar Purkinje cells *in vivo*

Curiously, the intensity of calbindin labelling in Purkinje cells was noteworthy diminished in FXN-deficient cerebellar neurons compared with sham cerebellar neurons or cerebellar neurons transduced with the lentivector shRNA-sc (Figure 7a). In parallel, calbindin 28k protein level as measured by western blot was significantly decreased in FXN-deficient cerebella, and this decline was prevented when BDNF was overexpressed (Figure 7b,c). When FXN-deficient cerebella were cotransduced with HSV-BDNF no significant loss of calbindin in Purkinje cells was noticed. These results indicated that the *in vivo* administration of HSV-BDNF prevented the loss of calbindin in Purkinje

cells in the cerebellum of mice which is caused by the deficiency of FXN.

BDNF prevents the development of ataxia in mice with FXN gene knockdown

To test for the functional effect of BDNF gene transfer on FXN knockdown, we evaluated the motor coordination of trial mice using the rota-rod test. First, we wanted to test whether the injection of shRNA37 in the animals had an effect on their motor coordination. The performance of the animals in the shRNA-37 group in the rota-rod test was significantly reduced 2 weeks after the surgery in comparison with those injected with shRNA-sc and sham animals (Figure 8b). To examine whether the neuroprotection offered by HSV-BDNF was sufficient to protect against altered motor coordination, we analyzed the motor activity with the rota-rod test as well. By the end of the second week animals injected with shRNA-37 and HSV-LacZ worsened in rota-rod test. Interestingly, however, when the shRNA-37 animals were cotreated with HSV-BDNF, their score in the rota-rod test significantly improved. These differences were maintained over 5 weeks after the operation (Figure 8b). In summary, these data support the idea that the neurological defects caused by the FXN depletion in the cerebellum can be prevented by BDNF gene transfer.

DISCUSSION

Here, we provide a proof of principle about the potential therapeutic value of using viral vector-mediated neurotrophin gene transfer to protect FXN-deficient neurons from degeneration. As an experimental tool to generate FXN-deficient neurons, a lentiviral vector encoding for a FXN-specific shRNA has been used both

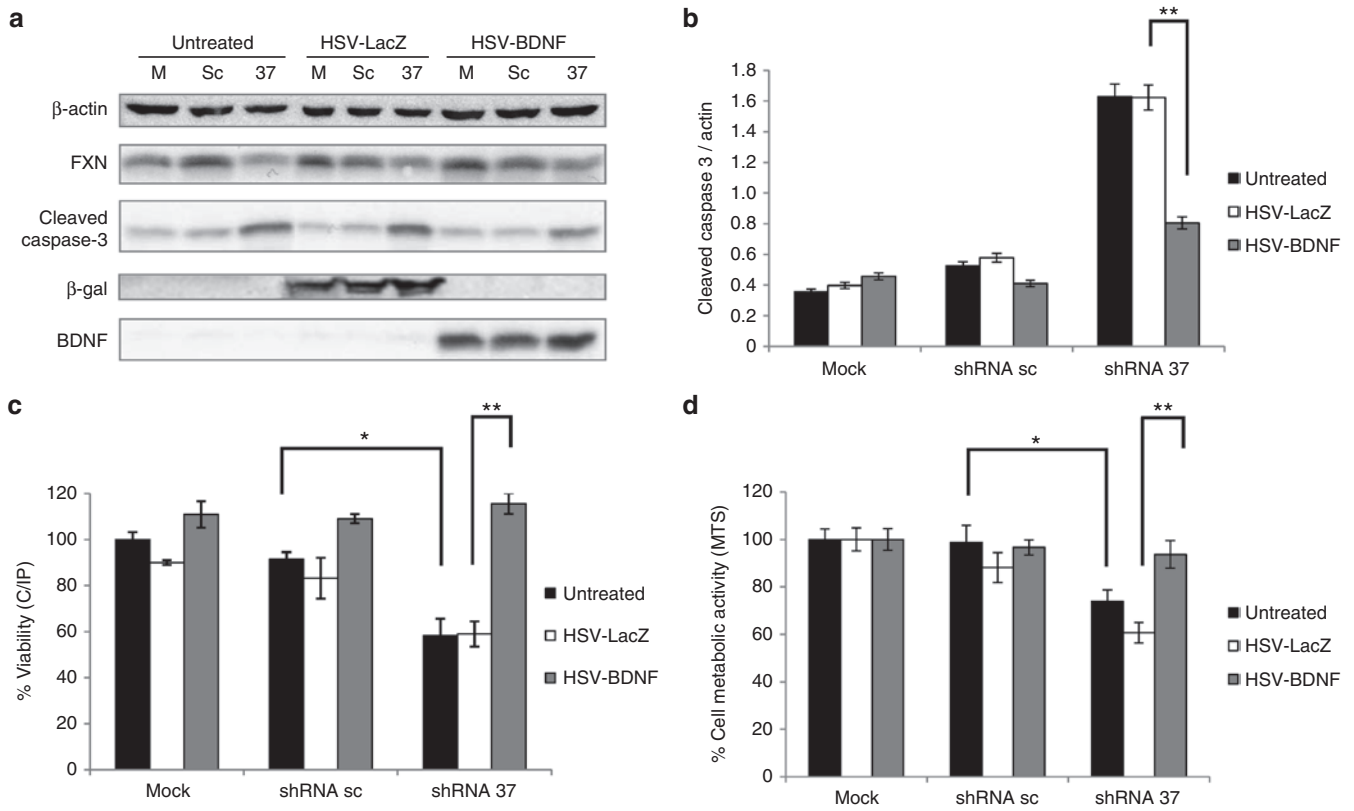


Figure 3 BDNF gene transfer prevents apoptotic cell death of FXN-deficient neurons in culture. Primary cortical neurons were transduced with lentivectors (shRNA-sc or shRNA-37) or were left untransduced as a mock control (m), in the presence of HSV-1 amplicon vectors containing the cDNA of BDNF (HSV-BDNF) or the cDNA of β -galactosidase (HSV-LacZ) as control. **(a)** Representative western-blot analysis of FXN, cleaved caspase-3, β -galactosidase, and BDNF levels at 72 hours upon cotransduction. **(b)** Quantification of cleaved caspase-3 levels in FXN-deficient neurons upon cotransduction reveals a decrease of caspase-3 activation when BDNF was overexpressed. **(c)** Cell viability of cultured neurons at 72 hours upon cotransduction as assessed by the calcein/propidium iodide assay shows significant differences between FXN-deficient neurons with or without HSV-BDNF. **(d)** Cell metabolic activity of cultured neurons at 72 hours upon cotransduction was assessed by MTS reduction and also shows significant differences between FXN-deficient neurons with or without HSV-BDNF. Data represent mean values \pm SEM from three independent experiments, $*P \leq 0.05$, $**P \leq 0.005$.

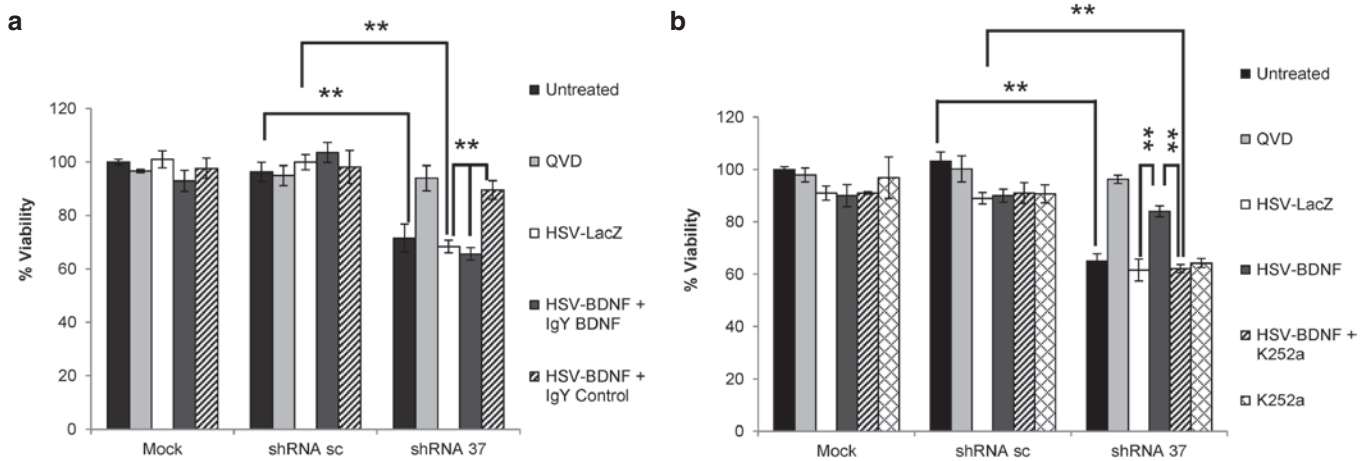


Figure 4 BDNF neuroprotective effect is mediated by TrkB receptor. Primary cortical neurons were cotransduced with lentivectors (shRNA-sc or shRNA-37) and HSV-1 amplicon vectors (HSV-LacZ or HSV-BDNF). **(a)** Cell viability assay of cultured neurons at 72 hours upon cotransduction shows significant difference in the presence of the BDNF neutralizing antibody or a control IgY antibody (20 μ g/ml) added to the media. **(b)** Cell viability assay of cultured neurons at 72 hours upon cotransduction shows significant difference in the absence or presence of 50 nM of TrkB inhibitor K252a. Data represent mean values \pm SEM from three independent experiments, $**P \leq 0.005$.

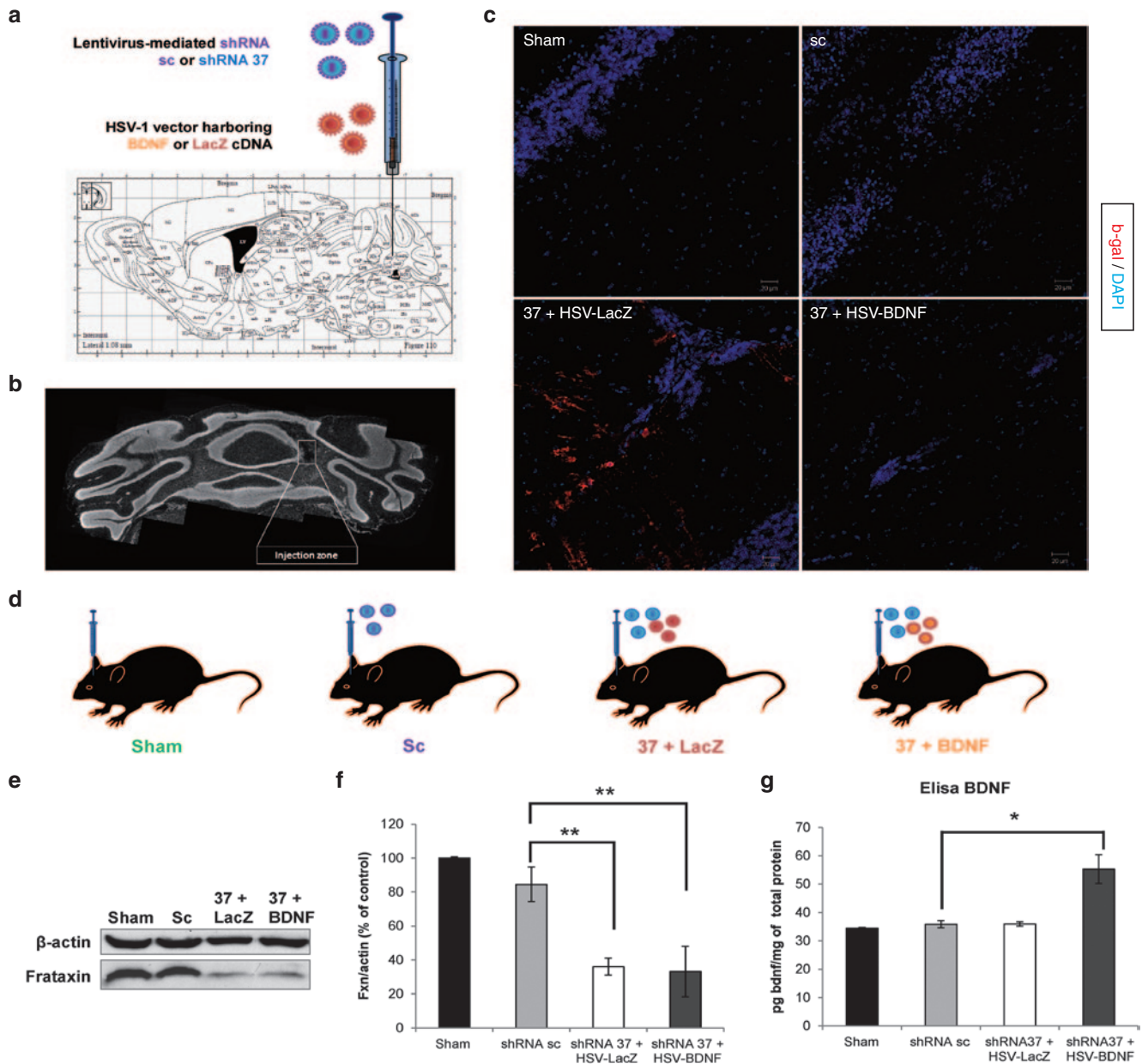


Figure 5 FXN knockdown and BDNF overexpression after stereotaxic injection of viral vectors into the cerebellum. 8-week-old male C57BL/6 mice were injected with lentivectors (shRNA-sc or shRNA-37) and HSV-1 amplicon vectors (HSV-LacZ or HSV-BDNF) by stereotaxic injection into the cerebellum. **(a)** Schematic sagittal section of mouse cerebellum at coordinates AP -6.5 mm; lateral 1 mm; V -2.5 mm.³⁹ **(b)** Coronal cerebellar section staining with nucleus marker 4'-6-diamidino-2-phenylindole (DAPI) (white) that indicates the region injected. Bar: 10 μ m. **(c)** Confocal images show representative staining of cells, after immunohistochemistry for β -galactosidase (red) and the nucleus marker DAPI (blue), in the cerebellar cortex of sham animals or treated with shRNA-sc or with shRNA-37 and HSV-LacZ or with shRNA-37 and HSV-BDNF. Cerebellar sections were from mice killed 4 days after injection. Bar: 20 μ m. **(d)** Scheme shows the four experimental groups of animals, *sham*, *sc*, *37 + HSV-LacZ*, and *37 + HSV-BDNF*. **(e)** Western-blot analysis of FXN levels in cerebella of mice 4 days after injection. **(f)** Densitometric analysis of the levels of FXN in cerebellum reveals a significant decrease in those animals injected with shRNA-37. **(g)** BDNF levels in cerebella of mice 4 days after injection were measured by enzyme linked immunosorbent assay ELISA. Data represent mean values \pm SEM from three independent experiments, * $P < 0.05$, ** $P < 0.005$.

in vitro in cultured neurons and *in vivo* into the mouse cerebellum.¹⁵ We have chosen this approach because we had previously found that this specific shRNA-37 was very efficient in decreasing FXN expression to levels close to those found in "early-onset" FRDA patients.¹⁵ Here, we show that the stereotaxic injection of the lentiviral vector encoding for shRNA-37 induces significant neuropathological changes in the cerebellar cortex including an

increased apoptosis of granule cells and a loss of calbindin in Purkinje cells. Moreover, the *in vivo* knockdown of FXN gene expression is accompanied by a moderate but significant loss of motor coordination of mice as assayed by the rota-rod test. These results emphasize the usefulness of targeted knockdown of FXN gene expression in selected regions of CNS to model the pathogenesis and test for therapeutic interventions for FRDA. Previously

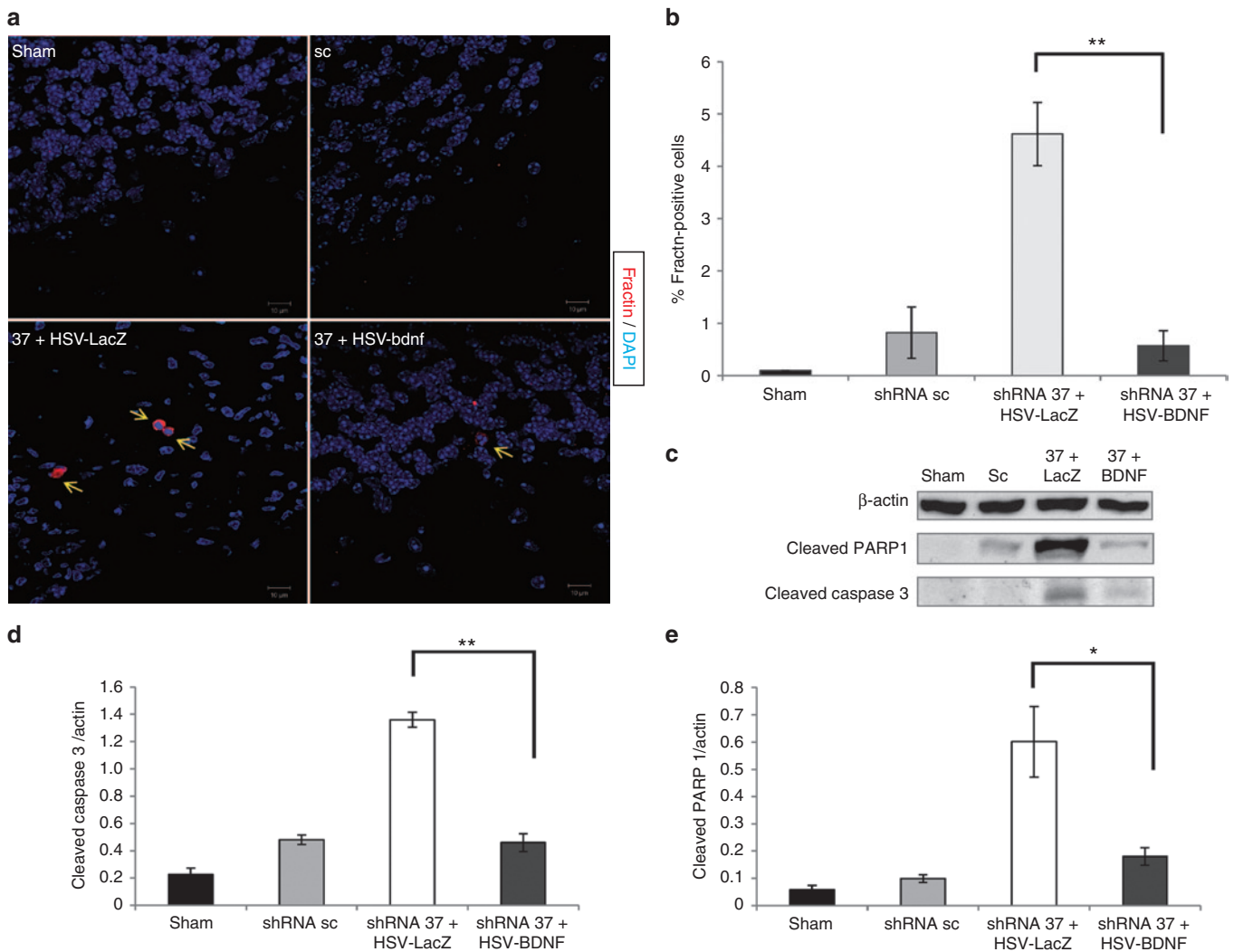


Figure 6 BDNF prevents apoptotic cell death of FXN-deficient cerebellar neurons *in vivo*. Animals were co-transduced with concentrated lentivectors (shRNA-sc or shRNA-37) and HSV-1 amplicon vectors (HSV-LacZ or HSV-BDNF) by *in vivo* stereotaxic injection into the cerebellum. **(a)** Confocal images show representative staining of cells after immunohistochemistry for fractin (red) and the nucleus marker DAPI (blue), in the cerebellum of sham animals or treated with shRNA-sc or with shRNA-37 and HSV-LacZ or with shRNA-37 and HSV-BDNF. Cerebellar sections were from mice killed 4 days after injection. Yellow arrows indicate positive cell for fractin. Bar: 10 μ m. **(b)** Quantification of fractin-positive cells in FXN-deficient cerebella indicated a significant decrease when BDNF was overexpressed compared with animals treated with HSV-LacZ. **(c)** Representative western-blot of PARP 1 and cleaved caspase-3 levels in cerebella of mice killed 4 days after injection. **(d)** Quantification of cleaved caspase-3 levels in FXN-deficient cerebella indicated a significant decrease when BDNF was overexpressed in comparison with animals treated with HSV-LacZ. **(e)** Quantification of cleaved PARP 1 levels in FXN-deficient cerebella indicated a significant decrease when BDNF was overexpressed compared with animals treated with HSV-LacZ. Data represent mean values \pm SEM from three independent experiments, * $P \leq 0.05$, ** $P \leq 0.005$.

other groups had demonstrated the potential of viral vectors for targeted overexpression of disease-causing proteins to model dominant spinocerebellar ataxias and other neurodegenerative diseases.^{41–43}

Our approach to modeling cerebellar neurodegeneration by knockdown of FXN expression using a lentiviral vector may be complementary to currently existing transgenic mouse models.¹⁴ Full FXN deletion mouse models generated by Cre-LoxP system exhibit a very early onset and drastic phenotype due to the complete absence of FXN in selected cell types, whereas GAA repeat expansion-based mouse models with residual FXN expression only exhibit a late onset, very mild and slowly progressive phenotype with no obvious cerebellar pathology.^{14,44–46} Our lentiviral

vector-based knockdown model may be an intermediate alternative as it triggers a fast development of a modest but significant ataxic phenotype. Thus, a decrease to 30% of FXN protein levels in the cerebellum of shRNA-37 injected animals is observed as early as 4 days after the operation. At the same time an increase of several apoptotic markers such as activated caspase 3, fractin, and cleaved PARP 1 is also observed. A significant decrease in the motor coordination of the shRNA-37 injected mice is only observed after 2 weeks from the operation, and this is maintained at least up to 5 weeks after operation. Possibly the delay between the appearance of the early apoptotic markers and the development of the ataxic phenotype is due to a requirement to pass a certain threshold of neurodegeneration. Both the neuropathology

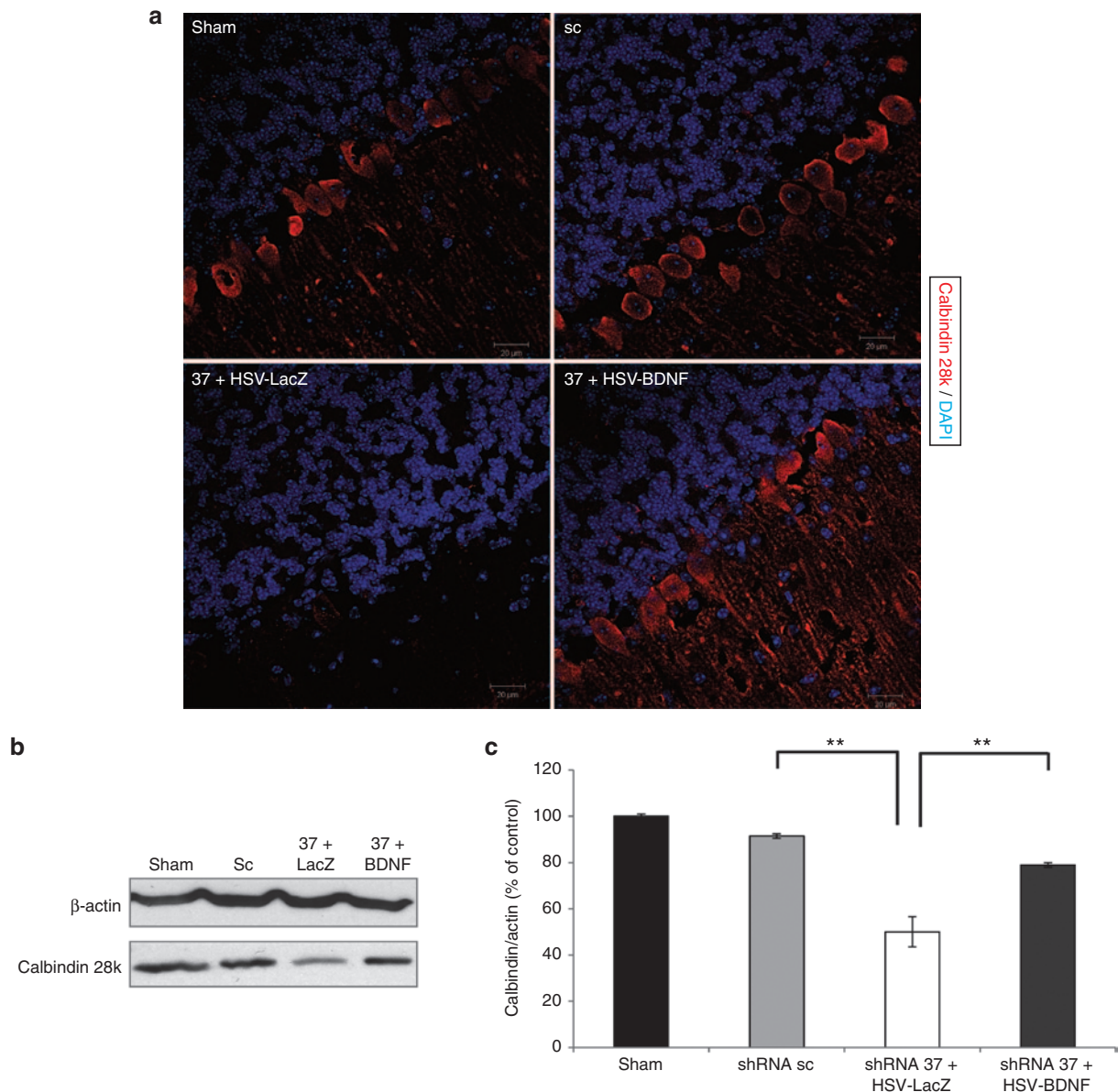


Figure 7 BDNF prevents the loss of calbindin in FXN-deficient cerebellar Purkinje cell *in vivo*. Animals were cotransduced with lentivectors (shRNA-sc or shRNA-37), and HSV-1 amplicon vectors (HSV-LacZ or HSV-BDNF) by *in vivo* stereotaxic injection into the cerebellum. **(a)** Confocal images show representative staining of cells, after immunohistochemistry for calbindin 28k (red) and the nucleus marker DAPI (blue), in the cerebellum of sham animals or treated with shRNA-sc or with shRNA-37 and HSV-LacZ or with shRNA-37 and HSV-BDNF. Cerebellar sections were from mice killed 4 days after injection. Bar: 20 μm. **(b)** Representative western-blot of calbindin 28k levels in cerebella of mice killed 4 days after injection. **(c)** Quantification of calbindin 28k levels in FXN-deficient cerebella indicated a significant increase when BDNF was overexpressed in comparison with animals treated with HSV-LacZ. Data represent mean values \pm SEM from three independent experiments, $**P \leq 0.005$.

and the time course of the behavioral phenotype of this model are very similar to a previously *in vivo* model characterized in our laboratory when HSV-CRE was injected into mice homozygous for a conditional *floxed* allele of the FXN gene.²⁴

An interesting feature of the cerebellar pathology found in our FXN knockdown model is the loss of calbindin in Purkinje cells. This may be a correlate of the atrophy of these neurons and has also been observed in a previously reported inducible conditional mouse model in which FXN deletion is restricted to neurons of dorsal root ganglia, spinal cord, and the cerebellum.⁴⁷ So it can be considered that loss of calbindin in Purkinje

cells is a marker of FXN deficiency in mouse models. However, these results are in marked contrast with previous pathological examinations of *post-mortem* cerebellar cortex from FRDA patients in which Purkinje cells appear normal as assessed by calbindin immunoreactivity.⁴⁸ A recent study has demonstrated that functional magnetic resonance imaging signal corresponding to head-movement-related activation is significantly reduced in the cerebellar cortex of FRDA patients (compared to matched controls) despite no or little structural changes revealed by MRI.⁴⁹ Thus, the cerebellar cortex of FRDA patients seems to be functionally affected even in the absence of a marked atrophy of

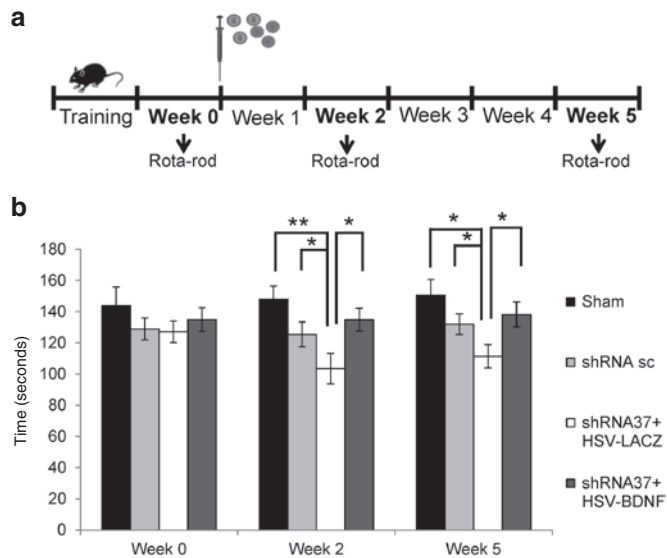


Figure 8 Rota-rod performance in FXN knockdown mice by *in vivo* stereotaxic injection of viral vectors into the cerebellum. Animals were co-transduced with lentivectors (shRNA-sc or shRNA-37) and HSV-1 amplicon vectors (HSV-LacZ or HSV-BDNF) by *in vivo* stereotaxic injection into the cerebellum. **(a)** Scheme of experimental procedure. **(b)** Mice were analyzed in the accelerating rota-rod test to measure motor activity and coordination, first before injection (week 0) and at 2 and 5 weeks after stereotaxic injection in the cerebellum. Data represent mean values \pm SEM from 10 mice, * $P \leq 0.05$, ** $P \leq 0.005$.

Purkinje cells, whereas these neurons became atrophic in mice when FXN deficiency is triggered by either viral vector-mediated knockdown (this study) or targeted disruption of the FXN gene.⁴⁷ It seems as if FXN deficiency might cause a subtle dysfunction of human Purkinje cells whereas it leads to a marked atrophy of mouse Purkinje cells. Of relevance in this regard are recent observations indicating that some of the differential neuronal susceptibility to disease that occurs in the human brain may have appeared recently during primate evolution. As a case in point, abundant lipofuscin deposition is observed in aged cerebellar Purkinje cells of many mammals except human and chimpanzees.⁵⁰ The reduced lipofuscin deposition probably reflects an increased resilience of human and chimpanzee Purkinje cells against oxidative stress.⁵⁰ This may explain why human Purkinje cells are less vulnerable than other neurons to a variety of pathological changes including aging-related lipofuscin deposition, intracellular inclusions in Fragile X-associated tremor ataxia syndrome patients, synuclein inclusions in Lewy body disease, and degeneration in FRDA.^{48,50-52} In view of these data, we suggest that rodent Purkinje cells may exhibit a more exaggerated response to FXN deficiency than human Purkinje cells, which has to be taken into account for the translational relevance of experimental studies performed in mice.

In this study, we have focused our attention on BDNF among the neurotrophic factor we have tested because of its greater potency to inhibit neuronal cell death triggered by FXN knockdown in primary cultures of mouse neurons. Moreover, BDNF TrkB receptors are widely expressed in the CNS including the cerebellum where BDNF seem to play important roles.⁵³⁻⁵⁵ Interestingly, TrkB receptors are particularly abundant not only in the cerebellar cortex but also in the deep cerebellar nuclei which

are very severely affected in FRDA.^{48,56} Furthermore, BDNF is particularly effective in promoting mitochondrial function which may be crucial for FRDA.^{3,12,57} In addition to BDNF, other neurotrophins like NT3 may be useful to target other specific neuronal populations like proprioceptive sensory neurons which are also affected in FRDA.³ Little is known about the status of neurotrophins and their receptors in FRDA. A recent report has described an upregulation of BDNF in periodontal ligament cells from FRDA patients compared to cells from healthy subjects.⁵⁸ However, we have failed to detect any significant change in BDNF in an analysis of the secretome of FXN-deficient astrocytes.¹⁷ So further research is required to clarify whether or not there are alterations in neurotrophins in neurons and astrocytes in FRDA.

Neurotrophic factors including BDNF may also be useful to slow down neuroinflammatory responses which might play a role in neurodegeneration in FRDA and other neurodegenerative diseases. Several studies have emphasized that FXN-deficient glial cells may trigger a neuroinflammatory response.^{17,59,60} Thus, BDNF has been demonstrated to reduce inflammation and apoptosis in an experimental model of allergic encephalomyelitis, as well as decreasing local inflammation in an experimental model of stroke.^{61,62} Interestingly, the overexpression of neurotrophic factors BDNF and FGF-2 after the intrahippocampal injection of HSV vectors attenuates epileptogenesis-associated neuroinflammation and prevents IL-1 β expression.⁶³ This latter effect may be of particular relevance for FRDA since it has been described an increased expression of IL-1 β in FXN-deficient Schwann cells.⁵⁹

Some previous observations support the view that neurotrophic factors may be useful for the therapy of FRDA. Application of recombinant insulin-like growth factor 1 (IGF-1) has been shown to normalize motor coordination in mildly ataxic FRDA-like transgenic mice.⁶⁴ In a proof-of-concept clinical trial, subcutaneous application of recombinant insulin-like growth factor 1 to a small number of FRDA patients appeared to decrease the progression of the disease.⁶⁵ Whereas a larger double-blind placebo-controlled trial is required to support this preliminary and promising observation, the systemic administration of recombinant proteins always gives rise to a transient effect which requires a continuing application. Targeted gene delivery to particular regions of the nervous systems may be a much more effective approach for long-term treatment of neurodegeneration. Cell transplantation has also been envisaged as a source of neurotrophic factors to treat neurodegenerative diseases. Thus, mesenchymal stem cells have been shown to secrete a variety of neurotrophic factors including BDNF and improve the motor coordination of mildly ataxic FRDA-like transgenic mice.^{66,67} However, a significant advantage of viral vector-mediated gene delivery over cell transplantation to provide neurotrophic factors is the possibility of fine-tuning neurotrophic factor gene expression using regulatable promoters.

For the delivery of the gene encoding BDNF, we have chosen an herpesviral amplicon vector because there is ample evidence about its suitability for neuronal gene transfer.^{37,68-72} In particular, HSV-1-derived amplicon vectors exhibit important advantages including their minimal toxicity, large capacity to accommodate therapeutic transgenes, widespread transduction of neural cells, and very low risk of insertional mutagenesis.⁶⁸ Targeted delivery of

neurotrophic factors to the primary sensory afferents for the treatment of neuropathology using viral vector-mediated gene transfer offers the possibility of highly selective targeted release of bioactive molecules within the nervous system.³⁷ Preclinical studies and clinical trials with nonreplicative HSV vectors injected into the skin to transduce neurons in the dorsal root ganglion (DRG) have demonstrated efficacy in preventing progression of sensory neuropathy without any systemic side effects.³⁷

In addition to promoting neuronal survival and function, neurotrophic factors may also enhance more direct gene replacement therapy as demonstrated in rodent models of retinal degeneration.⁷³ Thus, a combination of neurotrophic factor and gene replacement therapies may prove to be more useful than simple gene therapies. This may be relevant for FRDA. As FXN is an intracellular protein, only cells receiving a FXN gene may be “rescued” from the disease process. As neurotrophic factors are secreted proteins which may protect FXN-deficient neurons, the number of “rescued” neurons may be considerably larger than the number of “transduced” neurons receiving the therapeutic genes. Future research is required to test the synergy between FXN gene replacement and neurotrophic factor gene delivery.

In conclusion, we provide evidence for the therapeutic potential of neurotrophins like BDNF to treat neurodegeneration in FRDA. Viral vector-mediated gene encoding for neurotrophic factors may be therefore considered as an additional tool to current gene and cell therapy approaches which are now in progress.^{24,74,75}

MATERIALS AND METHODS

Reagents. Pan-caspase inhibitor Q-VD-OPh (*N*-(2-Quinolyl)-valyl-aspartyl-(2,6-difluorophenoxy)methyl ketone) and TrkB tyrosine kinase inhibitor k252a were obtained from Calbiochem EMD Biosciences (Merck KGaA, Darmstadt, Germany). BDNF neutralizing antibody (IgY isotype) and control IgY antibody were obtained from Promega (Madison, WI). Recombinant human trophic factors hepatocyte growth factor, nerve growth factor, neurotrophin-3, and neurotrophin-4 were obtained from Pepro Tech (Rocky Hill, NJ, EEUU), and BDNF were obtained from Alomone Labs (Jerusalem, Israel). The following antibodies were used for Western blot: polyclonal antisera against caspase-3 (1:1,000; Cell Signaling Technology, Danvers, MA); polyclonal antiserum against human FXN (R6.3s, 1:1,000) raised against the peptide TLGHPGSLDETTYERLAEETLC (Protein Tools, Madrid, Spain); monoclonal antibody against β -actin (1:2,000; Sigma, Madrid, Spain); polyclonal antiserum against β -galactosidase (1:5,000; MP Biomedical, Eschwege, Germany); polyclonal antiserum against BDNF (1:1,000; Santa Cruz Biotechnology, CA); monoclonal antibody against Poly [ADP-ribose] polymerase 1 (1:2,500; Sigma, Madrid, Spain); and polyclonal antiserum against Calbindin-D28K (1:1,000; Chemicon International, Temecula, CA). The following antibodies were used for immunohistochemistry: polyclonal antiserum against Calbindin-D28K (1:2,000; Chemicon International, Temecula, CA), polyclonal antiserum against β -galactosidase (1:1,000; Molecular Probes, Eugene, OR), and polyclonal antiserum against Fractin (1:500; Millipore Corporation, Billerica, MA).

Viral vectors. Lentiviral vectors encoding short-harpin RNA sequences were purchased from Sigma and contained either the sequences against human FXN (Mission[®] shRNA, Gene Bank accession number NM_000144), hereafter referred to as shRNA-37, or a nonspecific scrambled control (Mission[®] Non-Target shRNA, SHC002), hereafter referred to as shRNA-sc. Lentiviral packaging, stock production, concentration, and titration were performed as described previously.⁷⁶

HSV-1 were packaged using an improved HSV-1 helper-free system according to the protocol described previously.⁷⁷ The pHSVlac plasmid encoding the *Escherichia coli* β -galactosidase was used as reporter of gene transfer.⁷⁸ The pHSVbdfn amplicon vector has been described previously.^{79,80} Titters of HSV-1 amplicon stocks for both vectors were 7×10^5 IU/ml. HSV-1 amplicon vectors were packaged and used *in vitro* and *in vivo* in P2 facilities.

Neuronal cultures. Primary cultures of cortical neurons were established as described previously.⁸¹ 17-day-old C57BL/6 mice embryos were dissected in prechilled Hank's balanced salt solution (HBSS, Life Technologies, Barcelona, Spain). The cortices were cut and then incubated in a 0.25% trypsin (Sigma, Madrid, Spain), 1 mg/ml DNaseI (Roche, Barcelona, Spain) solution in Ca^{2+} and Mg^{2+} free HBSS for 15 minutes at 37 °C, shaking every 5 minutes. Trypsin and DNase were then eliminated by washing three times with HBSS, and then the tissue was homogenized using a siliconized pipette. The dissociated cells were counted and plated at a density of 1×10^5 cells/cm² onto poly-L-lysine precoated (1 mg/ml, Sigma, Madrid, Spain) dishes containing Neurobasal medium supplemented with 10% horse serum (both Invitrogen Life Technologies, Barcelona, Spain). After 3 hours, the medium was changed to neurobasal medium supplemented with 2% B-27, 2 mM GlutaMaxI (both Invitrogen Life Technologies, Barcelona, Spain), and a mix of penicillin and streptomycin (100 U/ml and 100 μ g/ml, respectively).

Cell viability. Cell viability was assessed by calcein-propidium iodide uptake.⁸² Calcein/acetoxymethyl ester is taken up and cleaved by esterases present in living cells, yielding yellowish-green fluorescence. In contrast, propidium iodide is taken up only by dead cells, which then exhibit orange-red fluorescence. Briefly, cells were incubated at 37 °C for 30 minutes with 8 μ M propidium iodide (Sigma, Madrid, Spain) and 1 μ M calcein/acetoxymethyl ester (Molecular Probes, Eugene, OR). The cells were visualized by fluorescence microscopy with a Zeiss Axiovert 135 microscope. Three randomly selected fields were analyzed per well (200–300 cells/field) in at least three independent experiments. Cell viability was expressed as the percentage of calcein-positive cells with respect to the total number of cells, for each experimental condition.

Cell metabolic activity. Cell metabolic activity was assessed with the CellTiter 96[®] AQueous One Solution Cell Proliferation Assay kit (Promega, Madison, WI) which is a colorimetric assay for assessing cell metabolic activity.⁸³ This assay kit contains a novel tetrazolium compound [3-(4,5-dimethylthiazol-2-yl)-5-(3-carboxymethoxyphenyl)-2-(4-sulfophenyl)-2H-tetrazolium, inner salt; MTS(a)] and an electron coupling reagent (phenazine ethosulfate). Phenazine ethosulfate has enhanced chemical stability, which allows it to be combined with MTS to form a stable solution. The MTS tetrazolium compound (Owen's reagent) is bioreduced by cells into a colored formazan product that is soluble in tissue culture medium. This conversion is accomplished by NADPH or NADH produced by dehydrogenase enzymes in metabolically active cells.⁸³ Briefly, cells were incubated at 37 °C for 90 minutes with 20 μ l CellTiter 96[®] AQueous One Solution Reagent and then recording the absorbance at 490 nm with a 96-well plate reader. The quantity of formazan product as measured by absorbance at 490 nm is directly proportional to the number of living cells in culture. Triplicates were analyzed in at least three independent experiments for each experimental condition.

Animals. 8-week-old male C57BL/6 mice (Charles River Breeding Laboratories, Barcelona, Spain) were used in this study and the mice were housed in a temperature-controlled room under a 12 hours light/12 hours dark cycle, with free access to food and water *ad libitum*.

Stereotaxic injection. Animals were randomly assigned to one of the following groups, *sham* (control, injected with vehicle), *sc* (shRNA-sc),

37 + *LacZ* (shRNA-37 and HSV-*LacZ*), and 37 + *BDNF* (shRNA-37 + HSV-*BDNF*). They were anesthetized using isoflurane and when they no longer demonstrated the footpad pinch reflex, were positioned in a Stoelting Lab StandardJ stereotaxic instrument fitted with a mouse gas mask (#51609; Stoelting, Wood Dale, IL) and a burr hole drilled at 1 mm right from the midline, 6.5 mm rostral from lambda. A 26-gauge needle with 30° bevel attached to a 10- μ l Hamilton syringe was aligned over the burr hole and then lowered into the brain to a depth of 2.5 mm from the surface of the skull. Injections of 6 μ l concentrated shRNA lentivector and HSV-1 amplicon vector were performed over 6 minutes, after which the needle was withdrawn slowly over 3 minutes.

After surgery, the incision was closed with sutures and the animals were allowed to recover separately before being returned to their cages.

Rota-rod test for motor coordination. Motor coordination was determined in a rota-rod apparatus (Ugo Basile, Italy). Animals were tested using the accelerating rotating rod protocol, which consisted in three consecutive trials with an acceleration from 4 to 40 rpm over 3 minutes followed by 2 minutes at maximum velocity. Latency was defined as the duration for which the mice were able to maintain their equilibrium on the accelerating rod until falling off, and was recorded in three consecutive trials. One week before the first measurement, the mice received three training sessions to familiarize them with the procedure. Data were collected on a weekly basis until 5 weeks after the surgery. The trial was terminated when mice fell from the apparatus or after a maximum of 5 minutes.

Western blot analysis. For protein extracts, cells were washed once with phosphate-buffered saline (PBS), placed on ice, and then homogenized in a buffer containing: 20 mM HEPES, pH 7.4; 100 mM sodium chloride; 100 mM sodium fluoride; 1% Triton X-100; 1 mM sodium orthovanadate; 5 mM EDTA; and the Complete™ protease inhibitor cocktail (Roche Diagnostics, Barcelona, Spain). After centrifugation at 16,000 \times g for 5 minutes at 4°C the soluble fraction was obtained for determining the protein content via Bradford assay, samples containing the same amount of protein were mixed with electrophoresis buffer containing sodium dodecylsulfate, boiled for 5 minutes, and separated by gel electrophoresis in the presence of sodium dodecylsulfate on 8–15% acrylamide gels. The proteins were then electrotransferred to nitrocellulose membranes (Schleider & Schuell, Dassel, Germany), following standard procedures, and the membranes were blocked with 10% nonfat dried milk in PBS 0.1% Tween-20. Then, blocked membranes were incubated overnight with primary antibodies diluted in blocking solution at 4°C. The filters were then rinsed at least three times in PBS 0.1% Tween-20 and incubated with the corresponding peroxidase-conjugated secondary antibody for 1 hour at room temperature. The immunoreactive proteins were visualized using an enhanced chemiluminescence detection system (Amersham Buckinghamshire, UK), and subsequent densitometric analysis was performed with an imaging densitometer (GS-710 model; Bio-Rad, Hercules, CA).

For the *in vivo* experiment, 4 days after surgery mice were anesthetized with CO₂ and decapitated. The cerebellum was homogenized with a microtube homogenizer in a RIPA buffer (Thermo Scientific, IL) and followed the same procedure as for cell extract preparation.

Immunohistochemistry. Mice were anesthetized with CO₂ and decapitated 4 days after surgery and the cerebella were immediately removed and fixed for 24 hours in 4% paraformaldehyde in 0.1 M PB (pH 7.4) at 4°C. The cerebella were cryoprotected in 10, 20, and then 30% sucrose gradient (24 hours each) and 20- μ m thick coronal cryostat sections were obtained after embedding in Tissue Tek (Sakura Finetek Europa, Zoeterwoude, The Netherlands). Sections were washed three times with PBS and incubated in blocking solution (PBS 0.2% Triton X-100, 3% BSA) followed by an overnight incubation at 4°C with the primary antibody diluted in blocking solution. After washing with PBS, sections were incubated for 1 hour at room temperature with donkey Alexa-conjugated secondary

antibody (Alexa-Fluor 555-conjugated). Following extensive washes, the sections were stained with 4'-6-diamidino-2-phenylindole (1:5,000; Calbiochem EMD Bioscience, Merck KGaA, Darmstadt, Germany) for 10 minutes. After washing, the sections were immediately mounted with Fluoromount-G (Southern Biotech Assoc., Birmingham, AL) and examined on a laser scanning confocal microscope (710LSM) coupled to a vertical AxioImager.M2 (Zeiss) microscope.

Enzyme-linked immunosorbent assay (ELISA). BDNF levels in the cerebellum were determined in all experimental groups using the Chemikine™ BDNF Sandwich ELISA Kit (Chemicon International, Temecula, CA). The assay was performed following the manufacturer's instructions. Standard and test samples were incubated overnight at 4°C in 96-well precoated dish with a polyclonal antibody against BDNF. Standard curves were generated using known amounts of the growth factor. The detection system included a biotinylated anti-BDNF monoclonal antibody detected with a streptavidin-HRP conjugated solution. The chromogenic substrate solution of tetramethylbenzidine was added to the plate and the reaction stopped by adding the Stop Solution provided in the kit. The color change generated by the oxidation–reduction reaction was measured using a plate reader set at a wavelength of 450 nm (DYNEX Opys MR). The standard curve for BDNF provided a linear plot of absorbance versus concentration, which was used to determine the concentration of BDNF in the samples.

Statistical analysis. Results are expressed as mean \pm SEM values, and at three independent experiments are represented in the figures. Statistical comparison of the data sets was performed using Student's *t*-test. The differences are presented with their corresponding statistical significances or *P* value, which is the probability that the observation in a sample occurred merely by chance under the null hypothesis. For *in vivo* experiments, all values were expressed as the mean \pm SEM and the statistical significance was evaluated by the Mann–Whitney nonparametric test when Levene's test for homogeneity of variances was significant. Each group consisted of 10 mice. Statistical significance was attributed when *P* \leq 0.05.

Ethics statement. All animal studies were performed with authorization from the animal experimentation and bioethics committees according to institutional guidelines for animal handling and research. All efforts were made to minimize the number and suffering of used animals.

ACKNOWLEDGMENTS

This work was supported by grants of the Spanish National Research Plan (SAF 2012–38042) and the Autonomous Government of Madrid (S2010/BMD-2331). Research at the authors laboratory is also supported by Friedreich Ataxia Research Alliance (FARA), Ataxia UK, FARA Ireland, Spanish FEDAES, GENEFA, Babel Family, Italian ASIA and Swedich BotaFA. We thank Filip Lim (Universidad Autónoma de Madrid) for his generous gift of pHSV-BDNF. The authors declare no conflict of interest.

REFERENCES

- Parkinson, MH, Boesch, S, Nachbauer, W, Mariotti, C and Giunti, P (2013). Clinical features of Friedreich's ataxia: classical and atypical phenotypes. *J Neurochem* **126(Suppl 1)**: 103–117.
- Delatycki, MB and Corben, LA (2012). Clinical features of Friedreich ataxia. *J Child Neurol* **27**: 1133–1137.
- Lynch, DR, Deutsch, EC, Wilson, RB and Tennekoon, G (2012). Unanswered questions in Friedreich ataxia. *J Child Neurol* **27**: 1223–1229.
- Marmolino, D (2011). Friedreich's ataxia: past, present and future. *Brain Res Rev* **67**: 311–330.
- Koeppen, AH and Mazurkiewicz, JE (2013). Friedreich ataxia: neuropathology revised. *J Neuropathol Exp Neurol* **72**: 78–90.
- Gatchel, JR and Zoghbi, HY (2005). Diseases of unstable repeat expansion: mechanisms and common principles. *Nat Rev Genet* **6**: 743–755.
- Bidichandani, SI, Ashizawa, T and Patel, PI (1998). The GAA triplet-repeat expansion in Friedreich ataxia interferes with transcription and may be associated with an unusual DNA structure. *Am J Hum Genet* **62**: 111–121.
- Yandim, C, Natisvili, T and Festenstein, R (2013). Gene regulation and epigenetics in Friedreich's ataxia. *J Neurochem* **126(Suppl 1)**: 21–42.

9. Koutnikova, H, Campuzano, V, Foury, F, Dollé, P, Cazzalini, O and Koenig, M (1997). Studies of human, mouse and yeast homologues indicate a mitochondrial function for FXN. *Nat Genet* **16**: 345–351.
10. Bulteau, AL, O'Neill, HA, Kennedy, MC, Ikeda-Saito, M, Isaya, G and Szewczak, LI (2004). FXN acts as an iron chaperone protein to modulate mitochondrial aconitase activity. *Science* **305**: 242–245.
11. Pastore, A and Puccio, H (2013). FXN: a protein in search for a function. *J Neurochem* **126**(r 1): 43–52.
12. Isaya, G (2014). Mitochondrial iron-sulfur cluster dysfunction in neurodegenerative disease. *Front Pharmacol* **5**: 29.
13. Evans-Galea, MV, Lockhart, PJ, Galea, CA, Hannan, AJ and Delatycki, MB (2014). Beyond loss of FXN: the complex molecular pathology of Friedreich ataxia. *Discov Med* **17**: 25–35.
14. Perdomini, M, Hick, A, Puccio, H and Pook, MA (2013). Animal and cellular models of Friedreich ataxia. *J Neurochem* **126**(Suppl 1): 65–79.
15. Palomo, GM, Cerrato, T, Gargini, R and Diaz-Nido, J (2011). Silencing of FXN gene expression triggers p53-dependent apoptosis in human neuron-like cells. *Hum Mol Genet* **20**: 2807–2822.
16. Igoillo-Estevé, M, Gurgul-Convey, E, Hu, A, Romagueira Bichara Dos Santos, L, Abdulkarim, B, Chintawar, S *et al.* (2015). Unveiling a common mechanism of apoptosis in β -cells and neurons in Friedreich's ataxia. *Hum Mol Genet* **24**: 2274–2286.
17. Loria, F and Diaz-Nido, J (2015). FXN knockdown in human astrocytes triggers cell death and the release of factors that cause neuronal toxicity. *Neurobiol Dis* **76**: 1–12.
18. Golde, TE (2009). The therapeutic importance of understanding mechanisms of neuronal cell death in neurodegenerative disease. *Mol Neurodegener* **4**: 8.
19. Strawser, CJ, Schadt, KA and Lynch, DR (2014). Therapeutic approaches for the treatment of Friedreich's ataxia. *Expert Rev Neurother* **14**: 949–957.
20. Pérez-Luz, S, Gimenez-Cassina, A, Fernández-Frías, I, Wade-Martins, R and Díaz-Nido, J (2015). Delivery of the 135 kb human FXN genomic DNA locus gives rise to different FXN isoforms. *Genomics* **106**: 76–82.
21. Gérard, C, Xiao, X, Filali, M, Coulombe, Z, Arsénault, M, Couet, J *et al.* (2014). An AAV9 coding for FXN clearly improved the symptoms and prolonged the life of Friedreich ataxia mouse models. *Mol Ther Methods Clin Dev* **1**: 14044.
22. Gimenez-Cassina, A, Wade-Martins, R, Gomez-Sebastian, S, Corona, JC, Lim, F and Diaz-Nido, J (2011). Infectious delivery and long-term persistence of transgene expression in the brain by a 135-kb iBAC-FXN genomic DNA expression vector. *Gene Ther* **18**: 1015–1019.
23. Perdomini, M, Belbellaa, B, Monassier, L, Reutenauer, L, Messaddeq, N, Cartier, N *et al.* (2014). Prevention and reversal of severe mitochondrial cardiomyopathy by gene therapy in a mouse model of Friedreich's ataxia. *Nat Med* **20**: 542–547.
24. Lim, F, Palomo, GM, Mauritz, C, Giménez-Cassina, A, Illana, B, Wandosell, F *et al.* (2007). Functional recovery in a Friedreich's ataxia mouse model by FXN gene transfer using an HSV-1 amplicon vector. *Mol Ther* **15**: 1072–1078.
25. Chapdelaine, P, Coulombe, Z, Chikh, A, Gérard, C and Tremblay, JP (2013). A potential new therapeutic approach for Friedreich ataxia: induction of FXN expression with TALE proteins. *Mol Ther Nucleic Acids* **2**: e119.
26. Li, Y, Polak, U, Bhalla, AD, Rozwadowska, N, Butler, JS, Lynch, DR *et al.* (2015). Excision of expanded GAA repeats alleviates the molecular phenotype of Friedreich's ataxia. *Mol Ther* **23**: 1055–1065.
27. Reichardt, LF (2006). Neurotrophin-regulated signalling pathways. *Philos Trans R Soc Lond B Biol Sci* **361**: 1545–1564.
28. Allen, SJ, Watson, JJ, Shoemark, DK, Barua, NU and Patel, NK (2013). GDNF, NGF and BDNF as therapeutic options for neurodegeneration. *Pharmacol Ther* **138**: 155–175.
29. Tuszynski, MH (2002). Growth-factor gene therapy for neurodegenerative disorders. *Lancet Neurol* **1**: 51–57.
30. Feigin, A and Eidelberg, D (2007). Gene transfer therapy for neurodegenerative disorders. *Mov Disord* **22**: 1223–8; quiz 1369.
31. Lim, ST, Airavaara, M and Harvey, BK (2010). Viral vectors for neurotrophic factor delivery: a gene therapy approach for neurodegenerative diseases of the CNS. *Pharmacol Res* **61**: 14–26.
32. Lu-Nguyen, NB, Broadstock, M, Schliesser, MG, Bartholomae, CC, von Kalle, C, Schmidt, M *et al.* (2014). Transgenic expression of human glial cell line-derived neurotrophic factor from integration-deficient lentiviral vectors is neuroprotective in a rodent model of Parkinson's disease. *Hum Gene Ther* **25**: 631–641.
33. Harvey, AR, Lovett, SJ, Majda, BT, Yoon, JH, Wheeler, LP and Hodgetts, SI (2015). Neurotrophic factors for spinal cord repair: which, where, how and when to apply, and for what period of time? *Brain Res* **1619**: 36–71.
34. Rodrigues, TM, Jerónimo-Santos, A, Outeiro, TF, Sebastião, AM and Diógenes, MJ (2014). Challenges and promises in the development of neurotrophic factor-based therapies for Parkinson's disease. *Drugs Aging* **31**: 239–261.
35. Cai, J, Hua, F, Yuan, L, Tang, W, Lu, J, Yu, S *et al.* (2014). Potential therapeutic effects of neurotrophins for acute and chronic neurological diseases. *Biomed Res Int* **2014**: 601084.
36. Galluzzi, L, Aaronson, SA, Abrams, J, Alnemri, ES, Andrews, DW, Baehrecke, EH *et al.* (2009). Guidelines for the use and interpretation of assays for monitoring cell death in higher eukaryotes. *Cell Death Differ* **16**: 1093–1107.
37. Chattopadhyay, M (2013). Targeted delivery of growth factors by HSV-mediated gene transfer for peripheral neuropathy. *Curr Gene Ther* **13**: 315–321.
38. Serres, F and Carney, SL (2006). Nicotine regulates SH-SY5Y neuroblastoma cell proliferation through the release of brain-derived neurotrophic factor. *Brain Res* **1101**: 36–42.
39. Paxinos, G and Franklin, KBJ (2004). *The Mouse Brain in Stereotaxic Coordinates*. Elsevier Academic Press San Diego, CA.
40. Kaufmann, SH, Desnoyers, S, Ottaviano, Y, Davidson, NE and Poirier, GG (1993). Specific proteolytic cleavage of poly(ADP-ribose) polymerase: an early marker of chemotherapy-induced apoptosis. *Cancer Res* **53**: 3976–3985.
41. Matsuzaki, Y, Oue, M and Hirai, H (2014). Generation of a neurodegenerative disease mouse model using lentiviral vectors carrying an enhanced synapsin I promoter. *J Neurosci Methods* **223**: 133–143.
42. Nóbrega, C, Nascimento-Ferreira, I, Onofre, I, Albuquerque, D, Conceição, M, Déglon, N *et al.* (2013). Overexpression of mutant ataxin-3 in mouse cerebellum induces ataxia and cerebellar neuropathology. *Cerebellum* **12**: 441–455.
43. Kirik, D and Björklund, A (2003). Modeling CNS neurodegeneration by overexpression of disease-causing proteins using viral vectors. *Trends Neurosci* **26**: 386–392.
44. Puccio, H, Simon, D, Cossée, M, Criqui-Filipe, P, Tiziano, F, Melki, J *et al.* (2001). Mouse models for Friedreich ataxia exhibit cardiomyopathy, sensory nerve defect and Fe-S enzyme deficiency followed by intramitochondrial iron deposits. *Nat Genet* **27**: 181–186.
45. Al-Mahdawi, S, Pinto, RM, Varshney, D, Lawrence, L, Lowrie, MB, Hughes, S *et al.* (2006). GAA repeat expansion mutation mouse models of Friedreich ataxia exhibit oxidative stress leading to progressive neuronal and cardiac pathology. *Genomics* **88**: 580–590.
46. Anjomani Virmouni, S, Ezzatizadeh, V, Sandi, C, Sandi, M, Al-Mahdawi, S, Chutake, Y *et al.* (2015). A novel GAA-repeat-expansion-based mouse model of Friedreich's ataxia. *Dis Model Mech* **8**: 225–235.
47. Simon, D, Seznec, H, Gansmuller, A, Cabelle, N, Weber, P, Metzger, D *et al.* (2004). Friedreich ataxia mouse models with progressive cerebellar and sensory ataxia reveal autophagic neurodegeneration in dorsal root ganglia. *J Neurosci* **24**: 1987–1995.
48. Koepfen, AH, Davis, AN and Morral, JA (2011). The cerebellar component of Friedreich's ataxia. *Acta Neuropathol* **122**: 323–330.
49. Stefanescu, MR, Dohnalek, M, Maderwald, S, Thürling, M, Minnerop, M, Beck, A *et al.* (2015). Structural and functional MRI abnormalities of cerebellar cortex and nuclei in SCA3, SCA6 and Friedreich's ataxia. *Brain* **138**: 1182–1197.
50. Gillissen, EP, Leroy, K, Yilmaz, Z, Kövari, E, Bouras, C, Boom, A *et al.* (2016). A neuronal aging pattern unique to humans and common chimpanzees. *Brain Struct Funct* **221**: 647–664.
51. Greco, CM, Hagerman, RJ, Tassone, F, Chudley, AE, Del Bigio, MR, Jacquemont, S *et al.* (2002). Neuronal intranuclear inclusions in a new cerebellar tremor/ataxia syndrome among fragile X carriers. *Brain* **125**: 1760–1771.
52. Hishikawa, N, Hashizume, Y, Yoshida, M and Sobue, G (2003). Clinical and neuropathological correlates of Lewy body disease. *Acta Neuropathol* **105**: 341–350.
53. Jones, KR, Fariñas, I, Backus, C and Reichardt, LF (1994). Targeted disruption of the BDNF gene perturbs brain and sensory neuron development but not motor neuron development. *Cell* **76**: 989–999.
54. Schwartz, PM, Levy, RL, Borghesani, PR and Segal, RA (1998). Cerebellar pathology in BDNF^{-/-} mice: the classic view of neurotrophins is changing. *Mol Psychiatry* **3**: 116–120.
55. Huang, EJ and Reichardt, LF (2001). Neurotrophins: roles in neuronal development and function. *Annu Rev Neurosci* **24**: 677–736.
56. Quartu, M, Serra, MP, Manca, A, Follesa, P, Ambu, R and Del Fiocco, M (2003). High affinity neurotrophin receptors in the human pre-term newborn, infant, and adult cerebellum. *Int J Dev Neurosci* **21**: 309–320.
57. Markham, A, Bains, R, Franklin, P and Spedding, M (2014). Changes in mitochondrial function are pivotal in neurodegenerative and psychiatric disorders: how important is BDNF? *Br J Pharmacol* **171**: 2206–2229.
58. Quesada, MP, Jones, J, Rodríguez-Lozano, FJ, Moraleda, JM and Martínez, S (2015). Novel aberrant genetic and epigenetic events in Friedreich's ataxia. *Exp Cell Res* **335**: 51–61.
59. Lu, C, Schoenfeld, R, Shan, Y, Tsai, HJ, Hammock, B and Cortopassi, G (2009). FXN deficiency induces Schwann cell inflammation and death. *Biochim Biophys Acta* **1792**: 1052–1061.
60. Hayashi, G, Shen, Y, Pedersen, TL, Newman, JW, Pook, M and Cortopassi, G (2014). FXN deficiency increases cyclooxygenase 2 and prostaglandins in cell and animal models of Friedreich's ataxia. *Hum Mol Genet* **23**: 6838–6847.
61. Makar, TK, Trisler, D, Sura, KT, Sultana, S, Patel, N and Bever, CT (2008). Brain derived neurotrophic factor treatment reduces inflammation and apoptosis in experimental allergic encephalomyelitis. *J Neurol Sci* **270**: 70–76.
62. Jiang, Y, Wei, N, Zhu, J, Lu, T, Chen, Z, Xu, G *et al.* (2010). Effects of brain-derived neurotrophic factor on local inflammation in experimental stroke of rat. *Mediators Inflamm* **2010**: 372423.
63. Bovolenta, R, Zucchini, S, Paradiso, B, Rodi, D, Merigo, F, Navarro Mora, G *et al.* (2010). Hippocampal FGF-2 and BDNF overexpression attenuates epileptogenesis-associated neuroinflammation and reduces spontaneous recurrent seizures. *J Neuroinflammation* **7**: 81.
64. Franco, C, Fernández, S and Torres-Alemán, I (2012). FXN deficiency unveils cell-context dependent actions of insulin-like growth factor I on neurons. *Mol Neurodegener* **7**: 51.
65. Sanz-Gallego, I, Torres-Alemán, I and Arpa, J (2014). IGF-1 in Friedreich's Ataxia—proof-of-concept trial. *Cerebellum Ataxias* **1**: 1–8.
66. Jones, J, Estrada, A, Redondo, C, Bueno, C and Martínez, S (2012). Human adipose stem cell-conditioned medium increases survival of Friedreich's ataxia cells submitted to oxidative stress. *Stem Cells Dev* **21**: 2817–2826.
67. Jones, J, Estrada, A, Redondo, C, Pacheco-Torres, J, Sierrol-Piquer, MS, Garcia-Verdugo, JM *et al.* (2015). Mesenchymal stem cells improve motor functions and decrease neurodegeneration in ataxic mice. *Mol Ther* **23**: 130–138.
68. Jerusalinsky, D, Baez, MV and Epstein, AL (2012). Herpes simplex virus type 1-based amplicon vectors for fundamental research in neurosciences and gene therapy of neurological diseases. *J Physiol Paris* **106**: 2–11.
69. Fink, DJ and Wolfe, D (2011). Gene therapy for pain: a perspective. *Pain Manag* **1**: 379–381.
70. Simonato, M, Bennett, J, Boulis, NM, Castro, MG, Fink, DJ, Goins, WF *et al.* (2013). Progress in gene therapy for neurological disorders. *Nat Rev Neurol* **9**: 277–291.
71. Glorioso, JC (2014). Herpes simplex viral vectors: late bloomers with big potential. *Hum Gene Ther* **25**: 83–91.
72. Guedon, JM, Wu, S, Zheng, X, Churchill, CC, Glorioso, JC, Liu, CH *et al.* (2015). Current gene therapy using viral vectors for chronic pain. *Mol Pain* **11**: 27.
73. Buch, PK, MacLaren, RE, Durán, Y, Balagany, KS, MacNeil, A, Schlichtebredre, FC *et al.* (2006). In contrast to AAV-mediated Cntf expression, AAV-mediated Gdnf

- expression enhances gene replacement therapy in rodent models of retinal degeneration. *Mol Ther* **14**: 700–709.
74. Lim, F and Diaz-Nido, J (2009). Gene therapy approaches to ataxias. *Curr Gene Ther* **9**: 1–8.
75. Evans-Galea, MV, Pébay, A, Dottori, M, Corben, LA, Ong, SH, Lockhart, PJ *et al.* (2014). Cell and gene therapy for Friedreich ataxia: progress to date. *Hum Gene Ther* **25**: 684–693.
76. Follenzi, A and Naldini, L (2002). HIV-based vectors. Preparation and use. *Methods Mol Med* **69**: 259–274.
77. Saeki, Y, Fraefel, C, Ichikawa, T, Breakefield, XO and Chiocca, EA (2001). Improved helper virus-free packaging system for HSV amplicon vectors using an ICP27-deleted, oversized HSV-1 DNA in a bacterial artificial chromosome. *Mol Ther* **3**: 591–601.
78. Geller, AI and Breakefield, XO (1988). A defective HSV-1 vector expresses *Escherichia coli* beta-galactosidase in cultured peripheral neurons. *Science* **241**: 1667–1669.
79. Alonso, MT, Lim, F, Nuñez, L, Represa, J, Giraldez, F and Schimmgang, T (1996). HSV-1 vector mediated transfer of BDNF into cerebellar granule cells. *Neuroreport* **7**: 3105–3108.
80. Goodman, LJ, Valverde, J, Lim, F, Geschwind, MD, Federoff, HJ, Geller, AI *et al.* (1996). Regulated release and polarized localization of brain-derived neurotrophic factor in hippocampal neurons. *Mol Cell Neurosci* **7**: 222–238.
81. Bartlett, WP and Banker, GA (1984). An electron microscopic study of the development of axons and dendrites by hippocampal neurons in culture. I. Cells which develop without intercellular contacts. *J Neurosci* **4**: 1944–1953.
82. Mattson, MP, Barger, SW, Begley, JG and Mark, RJ (1995). Calcium, free radicals, and excitotoxic neuronal death in primary cell culture. *Methods Cell Biol* **46**: 187–216.
83. Berridge, MV, Herst, PM and Tan, AS (2005). Tetrazolium dyes as tools in cell biology: new insights into their cellular reduction. *Biotechnol Annu Rev* **11**: 127–152.